Journal of Fluorescence, Vol. 2, No. 3, 1992

Packing of Phospholipid Vesicles Studied by Oxygen Quenching of Laurdan Fluorescence

Tiziana Parasassi[1,3] and Enrico Gratton[2]

Received May 6, 1992; revised September 25, 1992; accepted September 28, 1992

Steady-state fluorescence oxygen quenching experiments were performed on phospholipid vesicles where 2-dimethylamino-6-lauroylnaphthalene (Laurdan) was inserted. The quenching efficiency was found to be much higher in vesicles in the liquid-crystalline phase with respect to the gel phase, by a factor of about 50. Since the oxygen solubility in the two phospholipid phases can differ at most by a factor of 4 based on literature values, we concluded that oxygen diffusion must be responsible for the great difference in the quenching efficiency. A relatively high quenching efficiency was also found in vesicles composed of equimolar gel and liquid-crystalline phospholipids. Simulations were performed using the linear superposition of the properties of the pure phases to demonstrate that, in the case of vesicles composed of coexisting phases, the diffusional properties of oxygen in each phase are largely modified by the presence of the other. The addition of 10 mol% cholesterol to the gel phase rendered Laurdan fluorescence approximately as quenchable as in the equimolar mixture of the two phases. This result points out that molecules such as cholesterol, which introduce packing defects in the bilayer, favor oxygen diffusion. From the oxygen quenching experiments and using the properties of generalized polarization, the rate of Laurdan dipolar relaxation can be estimated.

KEY WORDS: Generalized polarization; Laurdan; oxygen; phospholipids; quenching.

INTRODUCTION

The packing and dynamics of phospholipids in membranes have received major attention during the past two decades. Among the spectroscopic methods used to determine lipid structure and dynamics are NMR,[4] EPR, and fluorescence. Physical properties of the phospholipid bilayer are of relevance for several physiological functions. The localization and transport of molecular oxygen in the cell are of primary importance for the cell metabolism. Several groups have addressed the problem of determining the oxygen concentration and diffusion in the lipid bilayer [1–8]. There is a general consensus that oxygen solubility in the lipid phase is higher than in water [2]. This conclusion is based on a comparison between oxygen solubility in water and that in hydrocarbons and on direct measurements of oxygen solubility in membrane suspensions. Oxygen solubility has been determined to be higher in membranes in the liquid-crystalline phase than in the gel phase [2].

EPR [7] and NMR [6] methods can provide information on oxygen solubility gradient along the membrane normal. It has been determined that oxygen is

[1] Istituto di Medicina Sperimentale, CNR, Viale Marx 15, 00137 Roma, Italia.

[2] Laboratory for Fluorescence Dynamics, University of Illinois at Urbana–Champaign, 1110 West Green Street, Urbana, Illinois 61801.

[3] To whom correspondence should be addressed at: Istituto di Medicina Sperimentale, Viale Marx 15, 00137 Roma, Italia.

[4] Abbreviations used: Laudran; 2-dimethylamino-6-lauroylnapthalene; DLPC; dilauroylphosphatidylcholine; DMPC; dimyristoylphosphatidylcholine; DPH; 1,6-diphenyl-1,3,5-hexatriene; DPPC; dipalmitoylphosphatidylcholine; TNS; *p*-toluidinyl-6-naphthalene sulfonic acid; PBS; phosphate-buffered saline solution; GP; generalized polarization; NMR, nuclear magnetic resonance; EPR; electron paramagnetic resonance.

1053-0509/92/0900-0167$06.50/0

almost absent in the polar head region [6], while its concentration increases along the hydrocarbon region, reaching a maximum in the deeper part of the membrane [6].

There is little agreement on the value of the partition coefficient of oxygen between the membrane and the aqueous phase and on the value of the diffusion coefficient of oxygen in the membrane. The reported values of the oxygen partition coefficient between water and membrane in the liquid-crystalline phase and at temperatures between 20 and 40°C vary from 2 to 6, depending on the measurement method and on the assumptions used to calculate the volume where the oxygen can reside. For example, exclusion from the polar heads region gives a higher partition coefficient [5]. In the gel phase; values for the partition coefficient range between 0.2 for DPMC below 10°C to about 2 for DMPC at 20°C [4]. Still, the reported values are subject to variation, depending on the method and assumptions used in their derivation. The diffusion coefficient for oxygen in membranes also varies depending on how it is measured, and it ranges between 10^{-5} and to 2×10^{-5} cm^2/s.

Among the methods used to measure oxygen solubility and diffusion is fluorescence oxygen quenching [1,3,9]. In a fluorescence quenching experiment, the results are generally analyzed using the Stern–Volmer quenching plot. The slope of this plot provides the product of the unquenched lifetime of the probe and of the bimolecular collisional rate. If the unquenched fluorescence lifetime is known, the bimolecular collisional rate can be related to the diffusion coefficient through the Smoluchowski–Einstein relationship. Generally, the interpretation of the fluorescence experiment proceeds via an assumption about oxygen solubility, necessary for determining the abscissa of the Stern–Volmer plot, followed by calculation of the diffusion coefficient from its slope. Among the probes used for fluorescence quenching experiments in membranes, are pyrene [3], TNS, and DPH [1]. The quenching of pyrene has been studied by Fischkoff and Vanderkooi in DMPC vesicles at 20°C [3]. The conclusion of this work is that oxygen can quench pyrene fluorescence in the membrane, and the derived diffusional coefficient for oxygen was 1.51×10^{-5} cm^2/s for DMPC at 37°C and 0.932×10^{-5} cm^2/s for DPPC at 37°C. For TNS and DPH a similar conclusion was also reached by Lakowicz [1].

In the present study we report oxygen quenching experiments on 2-dimethylamino-6-lauroylnaphthalene (Laurdan) fluorescence. Laurdan is a naphthalene derivative which has very different excitation and emission spectra in the gel and in the liquid-crystalline phase [10]. Also, Laurdan fluorescent moiety localizes in the glycerol backbone of phospholipids [10]. Laurdan fluorescent moiety is far enough from the membrane surface not to be influenced by the charge and the type of the polar residues of phospholipids [11]. In addition, the lauroyl residue exactly matches the phospholipid tail, causing a minimal perturbation of the membrane packing. Laurdan spectral sensitivity to the membrane physical state arises from dipolar relaxation processes. This phenomenon causes a large spectral red shift in a medium that can relax at a rate comparable to or faster than the fluorescence rate such as the liquid-crystalline phase. Instead, minimal relaxation is observed in the gel phase. This spectral shift due to dipolar relaxation adds to the Stokes shift, causing a large spectral displacement between the gel and the liquid crystalline phase. This very large difference between the relaxation rate of the gel and that of the liquid-crystalline phase prompted us to study the process of oxygen diffusion in these two phases with the aim of getting a better understanding of the origin of this large difference in the relaxation rates and how the relaxation process can be influenced by other molecules, such as cholesterol. Moreover, the analysis of our data using the concept of generalized polarization (GP) [10,11] and the change in lifetime of the probe caused by the quenching by oxygen should allow us to determine directly the rate of the relaxation process that causes the spectral shift using only steady-state measurements, as predicted by Equation 3 in Ref. 11.

METHODS

Materials and Sample Preparation

Dilauroyl- and dipalmitoylphosphatidylcholine (DLPC and DPPC, respectively) were from Avanti Polar Lipids, Inc. (Alabaster, AL). Cholesterol was from Sigma Chemical Co. (St. Louis, MO). Laurdan was from Molecular Probes, Inc. (Eugene, OR). Phosphate-buffered saline solution (PBS) was from Flow Laboratories (UK). Chloroform was spectroscopic grade.

Multilamellar phospholipid vesicles were prepared by evaporating under a nitrogen stream the appropriate amount of phospholipids and Laurdan solutions in chloroform. The remaining film was then resuspended in PBS, capped under nitrogen, warmed above the phospholipid transition temperature, and vortexed. The final concentration of the total phospholipids and of phospholipids plus cholesterol was 0.3 mM. The Laurdan final concentration was 0.5 μM. All operations were performed in the dark or under red light. Prior to measure-

ment, samples were deoxygenated by vigorous N_2 bubbling for at least 45 min.

Fluorescence Measurements

Fluorescence steady-state spectra and generalized polarization (GP) measurements were obtained using a photon counting spectrofluorimeter, Model GREG PC (ISS Inc., Champaign, IL), equipped with a xenon arc lamp and an oxygen pressure bomb, described in Ref. 12, holding a 2 × 2-cm cuvette and thermostated at 20°C by a circulating water bath. During measurements, samples were continuously stirred. The measurements in the absence of oxygen were performed in N_2 atmosphere. After the application of each value of oxygen pressure, the samples were allowed to equilibrate for 40 min in the dark. The GP value was measured as reported [10,11]:

$$GP = (B - R)/(B + R) \quad (1)$$

where B and R are emission intensities at 440 and 490 nm, respectively. To minimize the time of illumination under high oxygen pressure, the emission spectra were collected from 400 to 500 nm in about 20 s per spectrum.

Fluorescence lifetime measurements were performed using a K2 fluorometer (ISS Inc.) equipped with a xenon arc lamp. Excitation was 340 nm with an 8-nm bandwidth. Emission was observed through a Janos 375 cutoff filter. An additional bandpass filter, Corning 754, was used after the excitation monochromator. 2-2′-*p*-Phenylene*bis*(5-phenyl)oxazole (POPOP) in ethanol was used as the reference ($\tau = 1.35$ ns).

RESULTS

In vesicles composed of phospholipids in the liquid-crystalline phase (DLPC at 20°C) or of a mixture of 50 mol% gel in the liquid-crystalline phase (1:1 DLPC:DPPC at 20°C), Laurdan steady-state emission spectra show a progressive blue shift as the oxygen pressure increases. The emission spectra and the emission center of mass are reported in Figs. 1 and 2, respectively, as a function of oxygen pressure. Particularly, the red part of the emission spectrum, above 440 nm, shows a pronounced decrease in intensity (Fig. 1). Laurdan emission spectra in phospholipids in the gel phase (DPPC at 20°C) did not show appreciable spectral shift (Fig. 2). Also, in samples composed of 10 mol% cholesterol in DPPC, the Laurdan emission shape was not affected by oxygen pressure (Fig. 2).

In Fig. 3 we report the ratio between the total intensity of the deoxygenated samples, integrated over the emission spectrum from 400 to 500 nm, and the same total intensity at different oxygen pressures (I_0/I). The higher slope is obtained with DLPC. The DPPC sample shows very little decrease in intensity as a function of oxygen pressure. The 50% mixture of the two phospholipids shows an intermediate behavior. In the sample containing 10 mol% cholesterol in DPPC, the decrease in the emission intensity vs oxygen pressure is similar to that in the 1:1 mixture.

A biphasic behavior can be observed in the sample composed of 50 mol% DPPC in DLPC (Fig. 3B). At low oxygen pressures, up to 100 psi, the slope of the Stern–Volmer plot and of the center of mass as a function of oxygen pressure is larger than that at higher oxygen pressure, from 200 to 1000 psi. The Stern–Volmer constants, K_{SV}, obtained from the above samples are summarized in Table I.

Laurdan GP values, calculated following Eq. [1], have been measured in the same samples using emission wavelengths of 440 and 490 nm and excitation wavelengths of 340 or 410 nm (Fig. 4). In agreement with the decrease in the red part of the emission spectrum, as the oxygen pressure increases, the GP value increases. The increase in GP value is faster using an excitation wavelength of 410 nm (Fig. 4B), compared to the increase in GP value obtained using excitation at 340 nm (Fig. 4A). This behavior was not observed in samples of pure DPPC or of DPPC with 10 mol% cholesterol.

For a better understanding of the biphasic behavior of the 1:1 mixture, simulations have been performed (Fig. 5), using the values of the pure DLPC and DPPC components and taking into account the different contribution to the total intensity of the two components in a mixed phase. The fractional intensity of one component with respect to the other has been calculated from Laurdan measured lifetime values in the pure DLPC and in the pure DPPC, which are 4.0 and 5.9 ns, respectively. Compared to the experimental results, the simulated emission spectra show a reduced blue shift and a slower decrease in the intensity of the red part of the emission spectra as the oxygen pressure is increased (Fig. 5). The exact biphasic behavior of the 1:1 mixture cannot be quantitatively reproduced in the simulated data.

To evaluate the rate of dipolar relaxation using the steady-state GP, we use the following equation, which is formally equivalent to the Perrin equation for polarization, as noted previously [11]:

$$\frac{B - R}{GP} - (B + R) = \frac{2b_o}{a_o - b_o}\left(1 + \frac{k_{ba}}{\Gamma}\right) \quad (2)$$

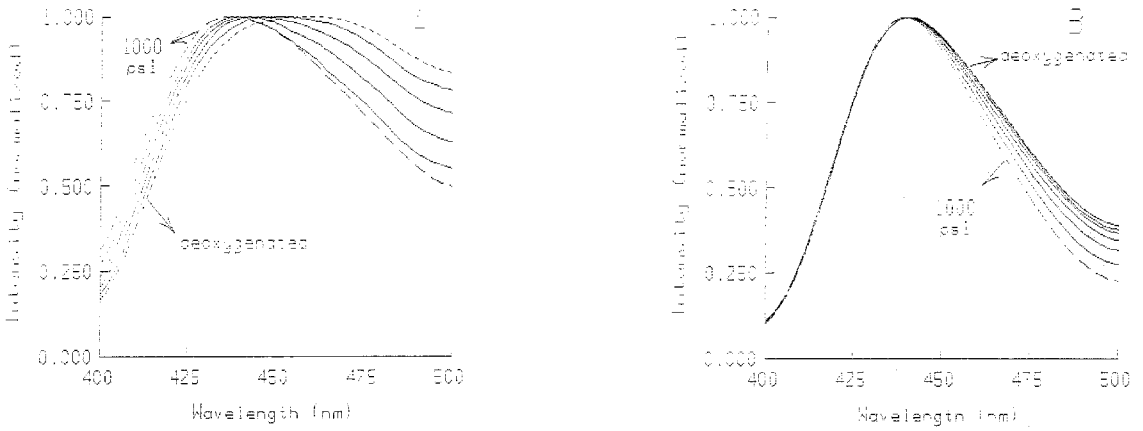

Fig. 1. Laurdan fluorescence emission spectra as a function of the oxygen pressure in DPLC vesicles (A) and vesicles composed of 50 mol% DPPC in DLPC (B). Measurements at 20 °C. Excitation at 340 nm. Excitation and emission bandwiths of 8 nm.

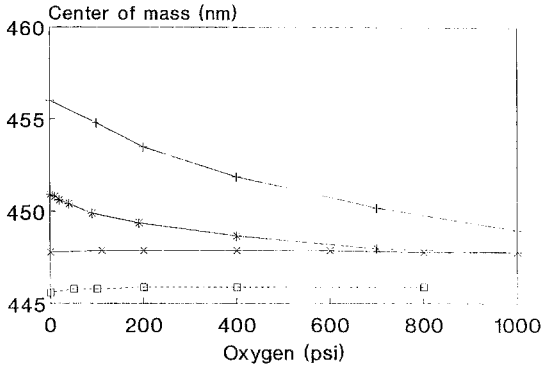

Fig. 2. Center of mass of Laurdan fluorescence emission spectra vs oxygen pressure, at 20 °C, in vesicles composed of DLPC (+), 50 mol% DPPC in DLPC (*), DPPC (×), and 10 mol% cholesterol in DPPC (□).

where a_o and b_o are the relative absorptions of the unrelaxed and relaxed species, B and R are the relative emission intensities of the unrelaxed species, in the blue at 440 nm and in the red at 490 nm, k_{ba} is the relaxation rate, and Γ is the decay rate. A plot of 1/GP vs 1/Γ gives a slope of

$$\frac{2b_o}{a_o - b_o} \times \frac{k_{ba}}{(B - R)} \tag{3}$$

from which k_{ba} can be estimated since the absorption and emission spectra of the relaxed and unrelaxed species are known. Perrin plots have been constructed for the pure DLPC and DPPC and for the 50% mixture, using

$$\tau/\tau_0 = 1/(1 + K_{SV}[O_2]) \tag{4}$$

where τ/τ_0 is the ratio between the lifetime value at a given oxygen concentration and the lifetime value in the absence of oxygen, K_{SV} is the value of the Stern–Volmer constant, and $[O_2]$ is the oxygen concentration. For the 1:1 mixture of the two phospholipids the value of $K_{SV} = 0.95 \times 10^{-3}$ obtained from the average slope of the Stern–Volmer plot has been used. Perrin plots obtained for the three samples are reported in Fig. 6. We have found that $k_{ba} \simeq 2.5 \times 10^9\ s^{-1}$ for the liquid-crystalline phase, and $k_{ba} \simeq 4 \times 10^7\ s^{-1}$ for the gel phase. The generalized Perrin equation assumes that the process of dipolar relaxation can be treated as a two-state process. Of course, this is a rough approximation, but the purpose here is to elucidate the order of magnitude of the relaxation rate and its difference between the gel and the liquid-crystalline phase.

DISCUSSION

The oxygen quenching experiments show a dramatic difference between the quenching of Laurdan in vesicles in the liquid-crystalline (DLPC) and that in the gel (DPPC) phase. The apparent Stern–Volmer constant differs by more than a factor of 50. There are several factors that can contribute to quenching. Oxygen has been demonstrated to be a collisional quencher with an efficiency of 1 per collision [13]. The overall quenching effect of the oxygen depends on its local concentration, the diffusion constant in the medium, and the lifetime of the fluorescent molecule. To compare the relative quenching effect on the gel with respect to the liquid-crystalline, we should know the relative solubility of

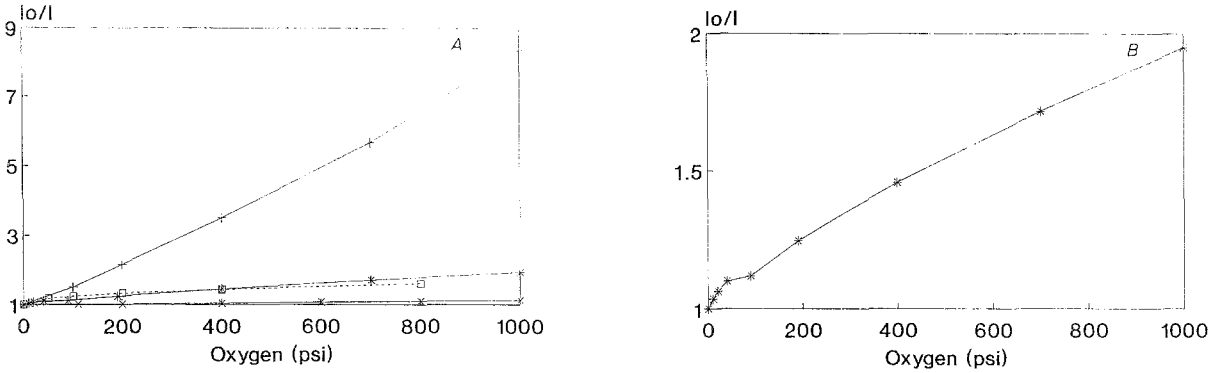

Fig. 3. (A) Stern–Volmer plot obtained with Laurdan in vesicles composed of DLPC (+), 50 mol% DPPC in DLPC (*), DPPC (×), and 10 mol% cholesterol in DPPC (□). The intensity represents the fluorescence integrated over the emission spectrum from 400 to 500 nm. Measurements at 20 °C. Excitation at 340 nm. Excitation and emission bandwiths of 8 nm. (B) The results obtained in vesicles composed of 50 mol% DPPC are reproduced on an enlarged scale.

Table I. Stern-Volmer Constants in Phospholipids Using Oxygen Pressure (psi)

	Slope	
Phospholipid	Initial	Average
DLPC		7.38×10^{-3}
50 mol% DPPC in DLPC	2.30×10^{-3}	0.95×10^{-3}
80 mol% DPPC in DLPC	1.67×10^{-3}	—
DPPC		0.13×10^{-3}
10 mol% cholesterol in DPPC		0.77×10^{-3}

oxygen in the two phase states. Generally, oxygen solubility in hydrocarbons is higher than in water, by about a factor of 4. With respect to solubility ratios between different phase states at the same temperature, previous estimates range between 2 and 4 in favor of the liquid-crystalline phase [2]. The lifetime of Laurdan in DLPC at 20°C is 4.0 ns, while in DPPC at 20°C it is 5.9 ns, which should make the gel phase more quenchable. Even if we account for the different partition coefficients of oxygen between the two phases, the observed difference in quenching can be due only to a large difference in the oxygen diffusion coefficient between the two phases. This difference should vary between a factor of at least 20 to a maximum of 100, depending on the estimate for the oxygen solubility in the two phases.

The diffusion constant of relatively large molecules such as pyrene-PC in the two phases has been measured, for example, recently by Sassaroli et al. [14] and by other researchers, in connection with the formation of pyrene excimers [15]. This rate has been estimated to

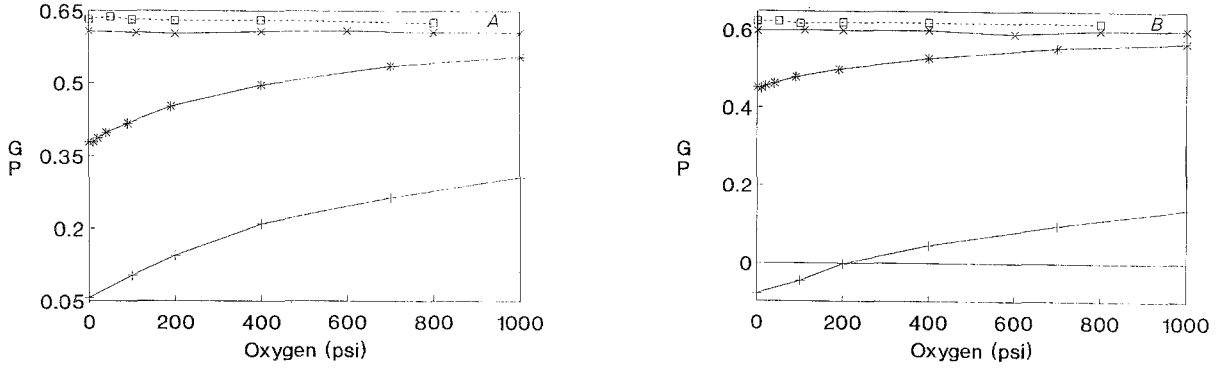

Fig. 4. Laurdan generalized polarization (GP) values as a function of oxygen pressure in vesicles composed of DLPC (+), 50 mol% DPPC in DLPC (*), DPPC (×), and 10 mol% cholesterol in DPPC (□). The GP value was obtained using emission intensities at 400 and 490 nm and excitation wavelengths of 340 nm (A) and 410 nm (B). Measurements at 20 °C. Excitation and emission bandwiths of 8 nm.

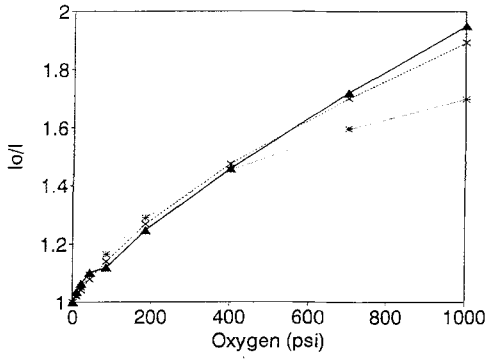

Fig. 5. Stern–Volmer plot obtained with Laurdan in vesicles composed of 50 mol% DPPC in DLPC. Solid line, experimental results; dotted line (*), simulation obtained as described in the text, using the Stern–Volmer constants obtained experimentally of $K_{SVg} = 0.13 \times 10^{-3}$ and $K_{SVl} = 7.38 \times 10^{-3}$; dashed line (×), simulation obtained using modified values of the Stern–Volmer constant of $K_{SVg} = 0.33 \times 10^{-3}$ and $K_{SVl} = 4.30 \times 10^{-3}$.

be approximately 18×10^{-8} cm²/s for pyrene-PC in the liquid-crystalline phase of DMPC at 25 °C and 9×10^{-8} cm²/s in the gel phase of DMPC at 15 °C [14]. Although the absolute value of the diffusion constant of oxygen and pyrene in the two phases cannot be compared due to the different sizes of the molecules, the relative value in the two phases should be similar. Deviations from Stokes–Einstein viscosity relationship has been observed previously for oxygen [16] but this deviation should tend to decrease the difference between the two phases. Therefore, our observation on the very large difference (20 to 100) of the quenching capability of oxygen in the two phases cannot be reconciled with the results obtained using excimer formation, which gives a difference of only a factor of 2 for the diffusion constant in the two phases. Either oxygen has a very different solubility in the DPLC than in DPPC, which is hard to explain on the basis of the chemical composition of the two phospholipids and on previous estimations, or oxygen diffusion in the gel phase is almost inhibited compared to the liquid-crystalline phase.

Instead, we note that the diffusion of large molecules (large compared to oxygen) differs by factors of more that 100 between the gel and the liquid-crystalline phase, when studied by fluorescence recovery after photobleaching (FRAP) methods [17–18]. Our results are in line with the FRAP observations and renders the discussion by Sassaroli *et al.* [14] regarding the reasons for the values of the diffusion coefficients obtained using pyrene excimer formation and FRAP technique quite questionable. This discussion is based on the difference

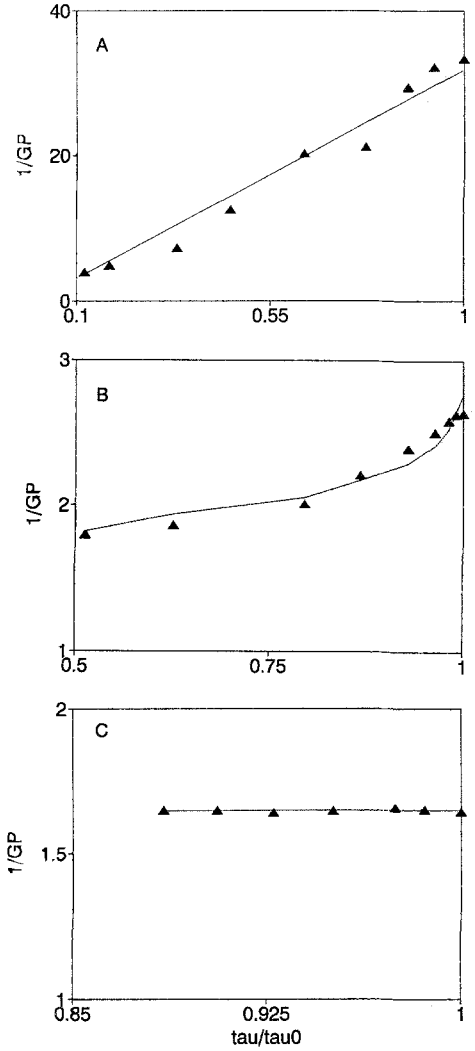

Fig. 6. Generalized Perrin Plot obtained from Laurdan GP values at different oxygen concentrations, as reported in the text, for vesicles composed of (A) DLPC, (B) a 1:1 mixture of DLPC:DPPC, and (C) DPPC.

between microscopic and macroscopic diffusion, but oxygen diffusion is microscopic in nature.

To reconcile the differences, one possibility is that the comparison with the diffusion of pyrene-PC is not valid and that this large molecule causes a profound perturbation of the membrane local structure that allows relatively fast diffusion. Instead, oxygen is very small and causes minimal perturbation, revealing the very tight packing of the pure gel phase.

To test this hypothesis further, we have analyzed the data of the 1:1 DLPC:DPPC mixture in order to estimate how the presence of DPLC can change the packing properties of the DPPC phase. We have previously shown that in this 1:1 mixture, there is phase coexistence, although the dynamical properties of the gel

and of the liquid-crystalline phase are modified [19]. In the present oxygen quenching experiments, phase coexistence is further demonstrated by the biphasic behavior of the Stern–Volmer plot of the 1:1 mixture (Fig. 3B). The slope of the Stern–Volmer plot is relatively high at low oxygen pressures, where quenching of Laurdan in the liquid-crystalline phase occurs preferentially. At higher oxygen pressures, quenching of Laurdan in the coexisting domain of gel phase also occurs, contrary to the virtual absence of quenching observed in the pure gel phase.

We have simulated a Stern–Volmer plot in which we assume that there are two coexisting phases at a 1:1 ratio. If in the simulation we use the Stern–Volmer constants, $K_{SVg} = 0.13 \times 10^{-3}$ and $K_{SVl} = 7.38 \times 10^{-3}$, for the gel and for the liquid-crystalline phase, respectively, we have the dotted line in Fig. 5. Instead, the best fit with the experimental results was obtained using the modified values of the Stern–Volmer constant of $K_{SVg} = 0.33 \times 10^{-3}$ and $K_{SVl} = 4.30 \times 10^{-3}$, for the gel and the liquid-crystalline phase, respectively. In other words, the two coexisting phases must have diffusional and/or solubility properties quite different from those of the pure phases. This observation is in line with our recent results on the modification of one phase caused by the presence of the other, obtained using time-resolved fluorescence methods [19].

We have used the same kind of approach of simulating other spectroscopic properties such as the shift of the center of mass as the oxygen pressure is increased. To assess further the extent of modification that one phase causes on the other, the GP plot was simulated, using the combination of the GP values obtained at the different oxygen pressures and at 20 °C for the pure components (not shown). Also in this case, the linear combination of the behavior of the two separate pure phases failed to reproduce the experimental observations of the 1:1 mixture. Instead, to fit the experimental observations we had to modify the spectroscopic properties of the gel to be more liquid-like and those of the liquid-crystalline to be more gel-like.

In general, the properties of the gel had to be more modified toward the liquid-crystalline than the properties of the liquid-crystalline toward the gel. This observation is in line with our suggestion that a small amount of DLPC in the DPPC phase can perturb the packing of the gel [19] to allow easier oxygen diffusion.

To study further the effect of packing on oxygen diffusion, we have conducted an experiment in which we added 10 mol% cholesterol to DPPC. This cholesterol concentration is considered to be relatively low compared to cholesterol physiological concentrations and insufficient to form a separate cholesterol phase [20]. In the presence of cholesterol, oxygen quenching was greatly enhanced, producing an apparent Stern–Volmer plot similar to that for the 1:1 DLPC:DPPC mixture. The well-established fluidization effect caused by cholesterol in the gel phase results in an enhanced oxygen diffusion which is likely to occur throughout the introduction of packing defects in the membrane.

In conclusion, oxygen quenching experiments on Laurdan in pure phospholipid phases reveal a very tight packing of the gel phase compared to the liquid-crystalline. This packing can be easily perturbed by the addition of other molecules such as DLPC and cholesterol, which produce defects that allow rapid oxygen diffusion. We have found a large difference between the parameters measured in the gel and those measured in the liquid-crystalline phase, differences that cannot be explained only by oxygen solubility effects. To explain our results we must assume a large difference in the diffusion coefficient of molecular oxygen in the two phases.

ACKNOWLEDGMENTS

We thank Dr. Beniamino Barbieri of ISS Inc. for providing the K2 fluorometer for lifetime measurements.

This work was supported by the CNR (T.P.) and NIH Grant RR03155 (E.G.).

REFERENCES

1. J. R. Lakowicz, F. G. Prendergast, and D. Hogen (1979) *Biochemistry* **18:** 520–527.
2. E. S. Smotkin, F. T. Moy, and W. Z. Plachy, (1991) *Biochem. Biophys. Acta* **1061**: 33–38.
3. S. Fischkoff, and J. M. Vanderkooi (1975) *J. Gen. Physiol.* **65:** 663–676.
4. W. K. Subczynski and J. S. Hyde (1983) *Biophys. J.* **41,** 283–286.
5. W. K. Subczynski and J. S. Hyde (1984) *Biophys J.* **45:** 743–748.
6. G. G. McDonald, J. M. Vanderkooi and J C. Oberholtzer (1979) *Arch. Biochem. Biophys.* **196:** 281–283.
7. K. Strzalka, T. Walczak, T. Sarna, and H. M. Swartz (1990) *Arch. Biochem. Biophys.* **281:** 312–318.
8. W. K. Subczynski, J. S. Hyde, and A. Kusumi (1991) *Biochemistry* **30:** 8578–8590.
9. M. Vauhkonen, M. Sassaroli, P. Somerharju, and J. Eisinger (1990) *Biophys. J.* **57:** 291–300.
10. T. Parasassi, G. De Stasio, A. d'Ubaldo, and E. Gratton, (1990) *Biophys. J.* **57:** 1179–1186.
11. T. Parasassi, G. De Stasio, G. Ravagnan, R. M. Rusch, and E. Gratton (1991) *Biophys. J.* **60:** 179–189.
12. J. R. Lakowicz and G. Weber (1973) *Biochemistry* **12:** 4161–4170.
13. W. R. Ware (1962) *J. Phys. Chem.* **66:** 455–468.

14. M. Sassaroli, M. Vauhkonen, D. Perry, and J. Eisinger (1990) *Biophys. J.* **57:** 281–290.
15. R. C. Hresko, I. P. Sugar, Y. Barenholz and T. E. Thompson (1986) *Biochemistry* **25:** 3813–3823.
16. J. Jordan, E. Ackerman and R. L. Berger (1956) *J. Am. Chem. Soc.* **78:** 2979–2982.
17. L. K. Tamm (1988) *Biochemistry* **27:** 1450–1457.
18. M. B. Schneider, W. K. Chan, and W. W. Webb (1982) *Biophys. J.* **43:** 157–165.
19. T. Parasassi, G. Ravagnan, R. M. Rusch and E. Gratton (1993) *Photochem Photobiol.* (in press).
20. M. B. Sankaram and T. E. Thompson (1990) *Biochemistry* **29:** 10676–10684.